International Journal of Mechanical, Industrial and Aerospace Sciences
ISSN: 2517-9950
Vol:4, No:9, 2010

Investigation of Tearing in Hydroforming Process with Analytical Equations and Finite Element Method

H.Seidi, M.Jalali Azizpour and S.A.Zahedi

***Abstract*—**Today, Hydroforming technology provides an attractive alternative to conventional matched die forming, especially for cost-sensitive, lower volume production, and for parts with irregular contours. In this study the critical fluid pressures which lead to rupture in the workpiece has been investigated by theoretical and finite element methods. The axisymmetric analysis was developed to investigate the tearing phenomenon in cylindrical Hydroforming Deep Drawing (HDD). By use of obtained equations the effect of anisotropy, drawing ratio, sheet thickness and strain hardening exponent on tearing diagram were investigated.

***Keywords*—**Hydroforming deep drawing, Pressure path, Axisymmetric analysis, Finite element simulation.

I. INTRODUCTION

HYDROFORMING Deep Drawing (HDD) is one of the metal forming processes that is used in industry to produce complex sheets with high Limiting Drawing Ratio (LDR). Schematic of cylindrical cup drawing with HDD process is shown in Fig.1. A pressurized fluid is employed in front of the workpiece. As the punch travels, the workpiece begins to deform into a cylindrical cup [1].

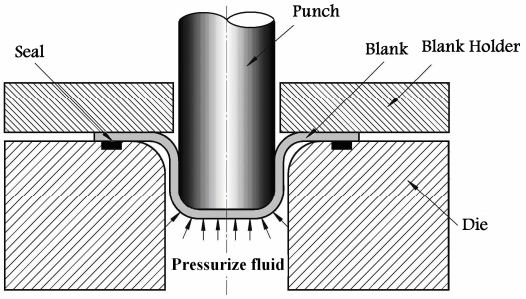

Fig.1. Hydroforming Deep Drawing (HDD) process

Some of the advantages of sheet hydroforming are improving the material formability, reduction of friction force, the accuracy of the forming part and the reduction of forming stages because of improvement of Limiting Drawing Ratio LDR [2]-[4].

Analysis of tearing phenomenon in hydroforming was studied by many researchers [5]-[8]. Generally, two kinds of material failure caused by inappropriate fluid pressure were identified. The failure by wrinkling at the lip area (The area that the blank is in contact with die and blank holder) results from insufficient fluid pressure, and the failure by rupture on the top of the cup results from excessive fluid pressure [9].

In this paper, a suitable punch-stroke pressure path was obtained theoretically that avoids rupture in HDD process. Finally effects of anisotropy, drawing ratio, sheet thickness and strain hardening in tearing diagram have been investigated.

II. PROBLEM FORMULATION

A number of assumptions that were made in this analysis are as below:

- The thickness of the workpiece remains constant throughout the process.
- The principal strain axes do not rotate.
- The Tresca yield criterion is satisfied and the fluid pressure p is smaller than the radial stress σ_r and the tangential stress σ_θ. This assumption yields $\sigma_r - \sigma_\theta = \sigma_e$.

For axisymmetric problems the polar equilibrium equation in the rim area is [10]:

$$\frac{d}{dr}(t\sigma_r)+\frac{t}{r}(\sigma_r-\sigma_\theta)+f(p)=0 \qquad (1)$$

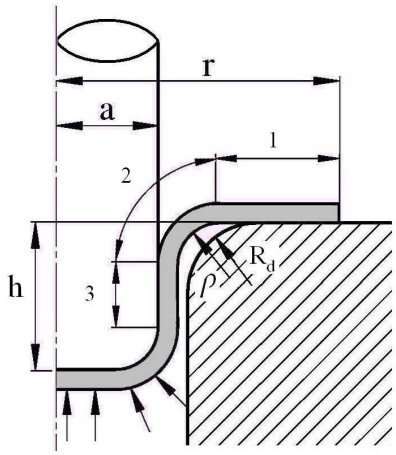

Fig. 2. Cylindrical sheet Hydroforming process

H.Seidi is with Islamic Azad University, Takestan branch. Iran. Email: hseidi@yahoo.com
M.Jalali Azizpour is with the production technology research institute, Ahwaz, Iran. Phone: +986113358491; fax: +986113358490; e-mail: m_jpour@yahoo.com
S.Abolfazl Zahedi is with Islamic Azad University, Juibar branch. Iran.

where $f(p)$ is the friction force in the rim area. By using the Tresca criterion and a power law for the material properties, Eq. (1) can be expressed as:

$$\frac{d}{dr}(t\sigma_r)+\frac{t}{r}(\sigma_0(\varepsilon_e)^n)+f(p)=0 \quad (2)$$

By using the normal anisotropy of the material in the formulation, the equivalent strain rate is denoted as

$$\varepsilon_e^{\bullet}=\frac{1+R}{\sqrt{1+2R}}[\varepsilon_r^{\bullet 2}+(\frac{2R}{1+R})\varepsilon_r^{\bullet}\varepsilon_\theta^{\bullet}+\varepsilon_\theta^{\bullet 2}]^{\frac{1}{2}} \quad (3)$$

Since it was assumed that the axis of strain does not rotate and by considering that the material follows volume constancy in the plastic deformation, the effective strain ε_e is obtained by integrating Eq. (3)

$$\varepsilon_e=\sqrt{R_e}\varepsilon_r \quad (4)$$

By substituting Eq. (4) into Eq. (2), we have

$$\frac{d}{dr}(t\sigma_r)+\frac{t}{r}(\sigma_0(R_e)^{\frac{n}{2}}\varepsilon_r^n)+f(p)=0 \quad (5)$$

Referring to Fig. 2 and substituting Eq. (5) for tension in area 1 we have

$$\sigma_r^{(1)}+\int_{r_0}^{r}\frac{\sigma_0(\mathrm{R}_e)^{n/2}(\varepsilon_r^{(1)})^n}{r}dr+\int_{r}^{b}\frac{f(p)}{t}dr= \quad (6)$$

By simplifying Eq. (6) for $\sigma_r^{(1)}$ we have

$$\sigma_r^{(1)}=\int_{r}^{b}\frac{\sigma_0(\mathrm{R}_e)^{n/2}(\varepsilon_r^{(1)})^n}{r}dr+\int_{r}^{b}\frac{f(p)}{t}dr \quad (7)$$

The value of strain in area 1 is obtained by

$$\varepsilon_r^{(1)}=\ln(\frac{G(r,h,p)}{r}) \quad (8)$$

Where:

$$G(r,h,p)=a\left\{\begin{matrix}1+(\frac{r}{a})^2-(1+\frac{\rho}{a})^2+\pi\frac{\rho}{a}(1+\frac{\rho}{a})\\-2(\frac{\rho}{a})^2+2(\frac{h}{a}-\frac{\rho}{a})Hv_{(\frac{h}{a}-\frac{\rho}{a})}\end{matrix}\right\}^{\frac{1}{2}} \quad (9)$$

Here $Hv_{(\frac{h}{a}-\frac{\rho}{a})}$ is Heaviside unit function.

In the same manner, the stress in area 2 is as follows:

$$\sigma_r^{(2)}=\sigma_{r\,(r=a+\rho)}^{(1)}+\int_{r}^{a+\rho}\frac{\sigma_0(\varepsilon_r^{(2)})^n R_e^{n/2}}{r}dr \quad (10)$$

In which the strain in area 2, $\varepsilon_r^{(2)}$, is

$$\varepsilon_r^{(2)}=\ln(\frac{F(r,h,p)}{r}) \quad (11)$$

Where $F(r,h,p)$ is:

$$F(r,h,p)=a\left\{\begin{matrix}1+2\frac{\rho}{a}(1+\frac{\rho}{a})(\frac{\pi}{2}-\beta)-\\2(\frac{\rho}{a})^2\cos\beta+2(\frac{h}{a}-\frac{\rho}{a})Hv_{(\frac{h}{a}-\frac{\rho}{a})}\end{matrix}\right\}^{\frac{1}{2}} \quad (12)$$

In Eq. (12), β is an angle shown in Fig.3 and is obtained by

$$\beta=\sin^{-1}(\frac{a+\rho-r}{\rho}) \quad (13)$$

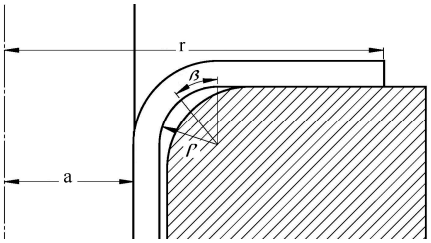

Fig 3. Geometry of β angle in analytical equations

If the bending stress is neglected and the radial stress σ_r is calculated for the pure radial drawing case, equilibrium of area (2) become:

$$\sigma_r^{(2)}(2\pi at)=P\pi[(a+\rho)^2-(a)^2] \quad (14)$$

III. Analysis of Tearing in Hydroforming Deep Drawing

Tearing usually occurs at the upper part of the punch; just at the beginning of drawn workpiece. It is caused by the firm contact between the workpiece and punch due to circumferential compressive fluid pressure [11]. This area is the transition between regions 2 and 3.The rate of tangential strain at the wall of the punch is zero. It means:

$$\varepsilon_\theta^{\bullet}=0 \quad (15)$$

By combining Eq. (15) and Eq. (3) below equation is achieved:

$$d\varepsilon_e^{(3)}=Zd\varepsilon_r^{(3)} \quad (16)$$

As predicted in reference 12, the instability of anisotropic material under biaxial plane strain conditions is as follows:

$$\frac{d\sigma_z}{d\varepsilon_e}=\frac{\sigma_e}{Z} \quad (17)$$

$$Z=\frac{(1+R)}{\sqrt{(1+2R)}} \quad (18)$$

So, if put Eq. (17) in Eq. (10) then

$$\sigma_{r\,critical}=\sigma_0\, n^n\, Z^{n+1} \quad (19)$$

Obviously, necking and rupturing occur when the radial load reaches a maximum value F_{max}:

$$F_{\max}=\sigma_r^{(3)}(r=a)t \quad (20)$$

By equating Eqs. (10) and (19) we have:

$$\sigma_0 n^n Z^{n+1} = \sigma_{r\,(r=a+\rho)}^{(1)} + \int_r^{a+\rho} \frac{\sigma_0(\varepsilon_r^2)R_e^{n/2}}{r} dr \qquad (21)$$

considering Eqs. (14) and (21) the fluid pressure causing rupture in the workpiece will be obtained. The material properties and the process parameters are given in Tables 1 and 2, respectively.

TABLE I
MATERIAL PROPERTIES

Material	St14
Thickness, t (*mm*)	1
Poisson ratio	0.3
Young's modulus, *E* (*GPa*)	210
Density, ρ (Kg/m^3)	7800
Isotropy, R	1

TABLE II
PROCESS CONDITIONS

Punch diameter, a (*mm*)	35
Blank diameter , b (*mm*)	75
Friction coefficient, μ	0.08
strain hardening exponent, n	0.27
σ_0 MPa	625

IV. FINITE ELEMENT METHOD

The commercial finite element software ABAQUS 6.8 was used for the simulation. The finite element model created in the software is shown in Fig. 4.

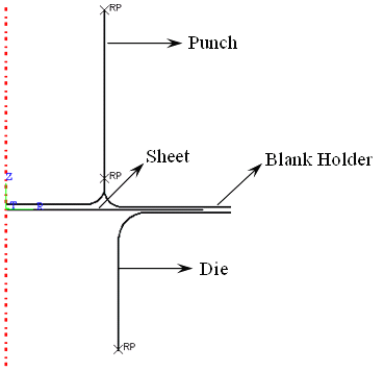

Fig. 4. The finite element model for the analysis of HDD in Abaqus software

In the simulations, the tools (punch, pressure chamber components and blank holder) were considered as rigid, while the sheet was considered to be deformable material. Coulomb friction equation was used to model the frictional condition between the blank and the tools. Due to symmetry, only half of the die and blank cross-section were modeled. In order to model the liquid, a uniform pressure distribution was used to apply the fluid pressure directly to the blank on the die opening. To introduce the pressure into the software use subroutine, called Vd load in ABAQUS, was used. The punch, die and blank holder were meshed with RAX2 (2-node linear axisymmetric rigid link for use in axisymmetric planar geometries) and the blank was meshed with SAX1 (2-node linear axisymmetric thin or thick shell).

In order to define the rupture diagram, several counter pressure–punch displacement were prescribed for the simulation. The rupture criterion used in this paper is the critical effective strain at instability [11], as follows:

$$\varepsilon_{cr} = nz \qquad (22)$$

$$z = \frac{1+R}{(1+2R)^{\frac{1}{2}}} \qquad (23)$$

V. RESULTS

The tearing diagrams obtained by the analytical equations and finite element method shown in Fig.5.

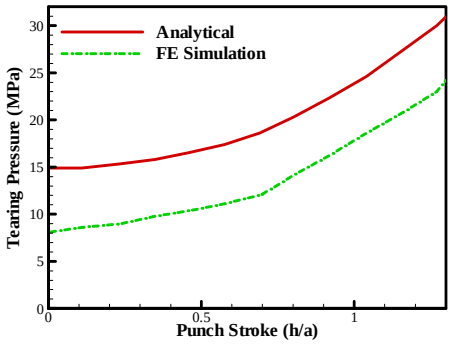

Fig. 5. Tearing diagram obtained from analytical approach and finite element simulation.

Both of the methods suggested that a counter-pressure history with a somewhat smaller pressurization at the initial stage and a larger one at the later stage would normally result in a proper cylindrical cup product. As illustrated in Fig. 5, the finite element simulation predicts limited zone compared with analytical equation. It means that analytical path is an upper limit to the tear diagram.

By using analytical equations, the effects of parameters in tearing diagram were understood easily that is shown in Fig. 6. This picture investigates the effects of anisotropy, drawing ratio, sheet thickness and strain hardening component on tearing diagram.

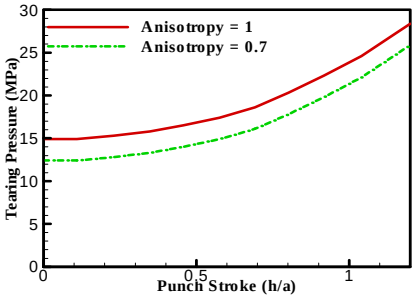

(a)

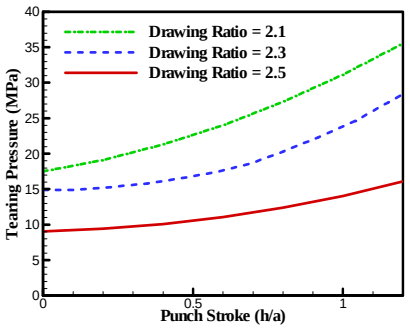

(b)

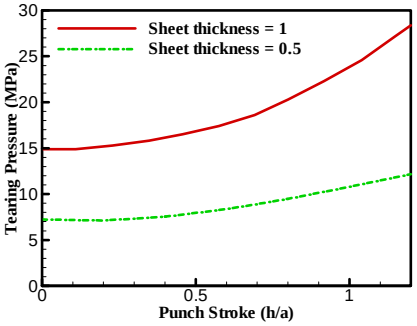

(c)

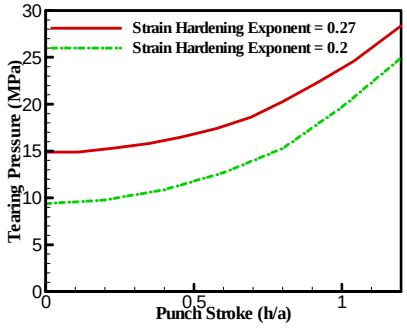

(d)

Fig. 6. Effect of a)Anisotropy, b)Drawing ratio, c) Sheet thickness, d)Strain hardening component on tearing diagram in HDD process

VI. Conclusion

The results of theoretical and finite element method of the HDD showed for product proper cylindrical cups. As it shown smaller pressurization at the initial stage and a larger one at the later stage should be used.

References

[1] Kandil. A, An experimental study of hydroforming deep drawing, *Journal of Material Processing Technology*, Vol. 134, No.1, 2003, pp. 70-80

[2] Oh. Soo-Ik, Byung-Hee Jeon , Hyun-Yong Kim, Jae- Bong Yang, Applications of hydroforming processes to automobile parts, *Journal of Material Processing Technology*, Vol. 174, No.1-3, 2006, pp. 42–55

[3] Parsa. M.H, P. Darbandi, Experimental and numerical analyses of sheet hydroforming process for production of an automobile body part, *Journal of Material Processing Technology*, Vol. 198, No. 1-3, 2008, pp. 381-390

[4] Lang. L, J. Danckert, K. Nielsen and X. Zhou, Investigation into the forming of a complex cup locally constrained by a round die based on an innovative hydromechanical deep drawing method, *Journal of Material Processing Technology*, Vol. 167, No. 2-3, 2005, pp. 191–200.

[5] Zhang. S.H, M.R. Jensen, J. Danckert, K.B. Nielsen, D.C. Kang and L.H. Lang, Analysis of the hydromechanical deep drawing of cylindrical cups", *Journal of Material Processing Technology*, Vol. 103, No. 3, 2000, pp. 367-373

[6] Lang. L, J, Danckert and K. Nielsen, Investigation into hydrodynamic deep drawing assisted by radial pressure Part II. Numerical analysis of the drawing mechanism and the process parameters, *Journal of Material Processing Technology*, Vol. 166, No. 1, 2005, pp. 150–161

[7] Dachang. K, C. Yu and X. Yongchao, Hydromechanical deep drawing of superalloy cups, *Journal of Material Processing Technology*, Vol. 166, No. 2, 2005, pp.243–246.

[8] Lang. L, T. Li, D. Ana, C. Chia, K. Nielsen and J. Danckert, Investigation into hydromechanical deep drawing of aluminum alloy Complicated components in aircraft manufacturing, *Material Science and England*, 2008, In press.

[9] Lo. Sy-wei, Tze-Chi Hsu and W. R. D. Wilson, An analysis of the hemispherical-punch hydroforming processe, *Journal of Material Processing Technology*, Vol. 37, No. 1-4, 1993, pp. 225-239.

[10] Tirosh. J and A. Hazut, The hydrodynamic deep-drawing process for blanks of non-uniform thickness, *International Journal of Mechanical Sciences*, Vol. 31, No. 2, 1989, pp. 121-130.

[11] Yossifon. S and J. Tirosh, Rupture instability in hydroforming deep-drawing process, *International Journal of Mechanical Sciences*, Vol. 27, No. 9, 1985,pp. 559-570..